8026 *Macromolecules* **2010**, *43*, 8026–8038
DOI: 10.1021/ma101490x

Macromolecules
ARTICLE

Hyperbranched−Linear Polyethylene Block Polymers Constructed with Chain Blocks of Hybrid Chain Topologies via One-Pot Stagewise Chain Walking Ethylene "Living" Polymerization

Yuanqing Xu,[†] Peng Xiang,[†] Zhibin Ye,*[,†] and Wen-Jun Wang[‡]

[†]*School of Engineering, Laurentian University, Sudbury, Ontario P3E 2C6, Canada, and* [‡]*State Key Lab of Chemical Engineering, Institute of Polymerization and Polymer Engineering, Department of Chemical and Biochemical Engineering, Zhejiang University, Hangzhou 310027, China*

Received July 5, 2010; Revised Manuscript Received August 25, 2010

ABSTRACT: We demonstrate in this article the facile synthesis of a novel range of "treelike" polyethylene block polymers constructed uniquely with chain blocks of hybrid hyperbranched−linear chain topologies from sole ethylene stock. Though chemically identical, the blocks in the polymers are featured with distinctly different chain topologies, varying from hyperbranched to linear. This synthesis is achieved uniquely through one-pot stagewise chain walking ethylene "living" polymerization with a Pd−diimine catalyst, [(ArN═C(Me)−(Me)C═NAr)Pd(CH_3)(N≡CMe)]$^+SbF_6^-$ (Ar = 2,6-(iPr)$_2$C$_6$H$_3$) (**1**), under varying conditions. It takes advantage of the combined outstanding features of the Pd−diimine catalyst in ethylene polymerization—the "living" polymerization behavior at a broad range of ethylene pressure and temperature and the capability of topology tuning by changing both parameters. In this stagewise "living" polymerization technique, the polymerization condition (ethylene pressure and temperature) is varied from stage to stage to grow blocks of different desired topologies while with maintained "living" behavior. With this technique, diblock polymers, containing a hyperbranched first block and a linear second block with controllable narrow-distributed sizes, have been obtained through two-stage polymerizations using the growth order of "hyperbranched-first" with the first stage at 1 atm/15 °C and the second stage at 27 atm/5 °C. The distinct block structure in these diblock polymers is verified based on the fact that their intrinsic viscosity data follow consistently the combination rule found with conventional diblock polymers. In addition, the synthesis of triblock polymers, composed of a hyperbranched first block, a medium-compact second block, and a linear third block, is also demonstrated through three-stage polymerization involving the first stage at 1 atm/15 °C, the second at 3 atm/15 °C, and the third at 27 atm/5 °C.

Introduction

The architecture/topology of a macromolecule is an important chain structural parameter that governs its physical properties and applications. The design and synthesis of polymers of complex, yet well-defined chain architectures have been a central theme in the research area of polymer science in the past two decades.[1] With the tremendous advancements in polymerization techniques, novel polymers with a rich variety of well-defined architectures/topologies, including dendrimers,[2] hyperbranched,[3] star,[4] and cyclic polymers,[5] have been successfully synthesized from various monomer stocks. Meanwhile, polymers having hybrid architectures, i.e., containing two or more different architectures in a single macromolecule, have also been developed. The most notable example is the "treelike" hybrid dendritic−linear block copolymers, which uniquely contain covalently jointed architecturally different dendritic (dendron or hyperbranched) and linear polymer blocks.[6] Combining the properties of both dendritic and linear polymers, hybrid dendritic−linear block copolymers with chemically distinct blocks have been demonstrated to have the interesting self-assembling feature and thus exhibit unusual solution and solid-state properties, which have encouraged their novel applications in such areas as drug delivery, catalysis, and thin film.[6−14]

The synthesis of hybrid dendritic−linear block copolymers often involves multistep strategies with the use of multiple monomer stocks. In particular, "living"/controlled polymerization techniques are often incorporated within the synthetic procedure in order to obtain well-defined narrow-distributed hybrid block polymers. Three synthesis strategies have been commonly adopted in the literature.[6] One strategy involves the coupling of preformed end-functionalized linear polymers with reactive dendritic architecture bearing a complementary functionality at the focal point.[6,7a,7b,12,14−16] Another strategy involves the divergent growth of dendron or hypergrafting of the hyperbranched block from a specially designed end-functionalized linear polymer.[6,7c,9,10a−10c,11,13,17,18] In the third strategy, dendritic molecules (dendrons or hyperbranched macromolecules) bearing a specific initiating site are used as the macroinitiator for the growth the linear polymer block via chain extension.[6,8,10d,19−23] Despite their elegance, these multistep synthetic strategies are often delicate and require sophisticated yet tedious polymer functionalization, purification, or separation procedures in each step.[6] The development of new one-pot polymerization strategies, which are convenient and facile while highly efficient in rendering the hybrid dendritic−linear polymers, is thus highly desired.

Tackling this challenge, we report in this article the synthesis of a novel class of hybrid hyperbranched−linear polyethylene block copolymers constructed with chemically identical polyethylene blocks of different chain topologies (hyperbranched and linear) through Pd−diimine-catalyzed chain walking ethylene "living" polymerization. In sharp contrast to above conventional strategies, the synthesis herein is accomplished uniquely in a one-pot

*Corresponding author: e-mail zye@laurentian.ca; Fax 1(705)675-4862.

 Published on Web 09/16/2010

Table 1. Single-Stage Ethylene Polymerizations (Runs 1−4) with Catalyst 1 at Four Different Combinations of Ethylene Pressure and Temperature and Polymer Characterization Results with Triple-Detection GPC and Melt Rheometry

				triple-detection GPC characterization[b]					melt rheometry characterization[c]	
run	ethylene press. and temp[a]	time (h)	polymer productivity (kg/(mol Pd h)	$M_{n,LS}$ (kDa)	$M_{w,LS}$ (kDa)	PDI_{LS}	$[\eta]_w$ (mL/g)	g'	η_0 (25 °C) (Pa s)	E_a (kJ/mol)
1	27 atm/5 °C	1	9.5	9.6	9.7	1.00	17.1	1.0	52	46
		2	6.4	17.4	17.5	1.01	23.5	1.0	295	48
		3	7.5	23.2	23.9	1.03	28.3	1.0	860	49
		4	6.7	29.1	30.3	1.04	32.3	0.99	1339	47
		5	7.0	34.1	36.0	1.06	36.0	1.0	2925	49
		6	6.9	38.5	41.9	1.09	39.0	0.99	5371	50
2	3 atm/15 °C	1	35	27.9	28.4	1.02	23.0	0.74	151	37
		2	20	40.4	42.1	1.04	28.5	0.72	499	45
		3		52.8	56.3	1.07	34.6	0.74	1591	49
		4		61.3	71.1	1.16	39.1	0.72	3362	49
		5	20	71.8	82.4	1.15	43.3	0.73	9453	53
		6	17	78.3	92.4	1.18	46.5	0.73	9946	53
3	1 atm/15 °C	0.5	13	9.0	9.0	1.00	9.9	0.63	11	40
		1	14	15.7	15.7	1.00	12.0	0.56	18	45
		2	14	28.0	28.6	1.02	17.5	0.56	39	41
		3	13	40.2	41.3	1.03	21.4	0.55	102	46
		4	13	50.4	53.5	1.06	25.1	0.55	192	46
		5	12	59.4	64.7	1.09	27.9	0.54	326	48
		6	13	64.7	74.1	1.14	30.3	0.55	464	49
4	1 atm/25 °C	1	30	27.3	28.2	1.03	14.5	0.47	25	46
		2	29	47.3	51.4	1.09	19.4	0.44	54	44
		3.2	26	63.2	74.1	1.17	23.9	0.43	97	46
		4	27	70.6	87.3	1.24	26.4	0.43	174	42
		5	28	78.1	101	1.29	28.9	0.43	231	45
		6	28	83.6	112	1.33	30.7	0.43	463	50

[a] Other polymerization conditions: amount of catalyst **1**, 0.32 mmol; solvent, chlorobenzene; total volume, 300 mL. [b] Number-average molecular weight ($M_{n,LS}$), weight-average molecular weight ($M_{w,LS}$), and polydispersity index (PDI_{LS}) are absolute values determined using the light scattering detector in triple-detection GPC. Weight-average intrinsic viscosity ($[\eta]_w$) data were measured using the online viscometer. The contraction factor (g') is defined as the ratio of intrinsic viscosity of the polymer to that of linear polymer of equal molecular weight synthesized at 27 atm and 5 °C. The fitting equation ($\log[\eta]_w = 0.603 \log M_w - 1.19$) shown in Figure 3 is used for the calculation of the intrinsic viscosity of the linear reference polymers of equal molecular weight. [c] Polymer melt rheological characterization was conducted in the small-amplitude dynamic oscillation mode within the linear viscoelastic region. The zero shear viscosity η_0 at 25 °C and flow activation energy (E_a) were obtained by evaluating the rheological data measured in the temperature range of 15−65 °C with time−temperature superposition.

process without requiring any intermediate polymer separation/purification steps. The success of this synthetic strategy benefits from the combined outstanding features of the Pd−diimine catalysts for ethylene polymerization, their "living" polymerization characteristics,[24−26] and chain walking mechanism.[27,28] Chain walking polymerization with Pd−diimine catalysts has been demonstrated to be a novel technique for the synthesis of polyethylenes of various controlled chain topologies, ranging from hyperbranched to linear structures, which exhibit interesting properties for novel applications.[27−31] In this technique, the control of polymer chain topology is achieved innovatively through the intrinsic chain walking mechanism of the Pd−diimine catalysts while with simple ethylene as the monomer. This differs distinctively from the conventional synthesis concepts/techniques for dendrimers and hyperbranched polymers, wherein the construction of the dendritic chain topology is often achieved through the use of specially designed multifunctional monomers.[2,3] Meanwhile, this technique also allows the convenient tuning of polymer topology from hyperbranched to linear by a simple adjustment of polymerization conditions, including ethylene pressure, temperature, and recently demonstrated chain-walking-blocking ring units.[27,28] In addition to polymer topology control, the Pd-catalyzed ethylene polymerization has also been demonstrated to exhibit typical "living" behavior at prescribed conditions, which has facilitated the synthesis of a range of polyethylenes of novel controlled architectures, including functionalized block copolymers, telechelic polymers, and star polymers.[24−26]

Utilizing the "living" polymerization feature along with the tunability of polymer topology via controlling polymerization conditions, we have designed and carried out herein chain walking ethylene "living" polymerization at varying conditions (ethylene pressure and temperature) for the synthesis of hybrid hyperbranched−linear polyethylene block polymers. During the course of "living" polymerization, the polymerization condition is varied to specifically tune the polymer topology in each block while without affecting the "living" polymerization characteristics. With this strategy, a range of hybrid block polymers constructed with topologically different while chemically identical blocks at controllable sizes have been successfully synthesized.

Experimental Section

Materials. The acetonitrile Pd−diimine catalyst used herein for ethylene polymerization, $[(ArN{=}C(Me){-}(Me)C{=}NAr)Pd(CH_3)(N{\equiv}CMe)]^+SbF_6^-$ (Ar = 2,6-(*i*Pr)$_2$C$_6$H$_3$) (**1**), was synthesized according to a literature procedure.[29d] Ultrahigh-purity N_2 (>99.97%) and polymer-grade ethylene (both from Praxair) were purified by passing through a 3 Å/5 Å molecular sieve column and an Oxiclear column in series to remove moisture and oxygen, respectively, before use. Chlorobenzene (99.5%, Aldrich) was refluxed over CaH_2 (powder, 90−95%, Aldrich) and distilled in a N_2 atmosphere before use. Other chemicals, including anhydrous dichloromethane (99.8%), triethylsilane (97%), methanol (>99%), tetrahydrofuran (THF) (>99%), toluene (≥99.5%), etc., were obtained from Aldrich and were used as received. In general, all manipulations involving air- and/or moisture-sensitive compounds were carried out in a N_2-filled glovebox or using the Schlenk technique.

General Procedure for Single-Stage Chain Walking Ethylene Polymerizations at a Single Constant Condition. The polymerizations (runs 1−4 shown in Table 1) were carried out in a 500 mL Autoclave Engineers Zipperclave reactor equipped with a MagneDrive agitator, a removable heating/cooling jacket, and a sampling port. The reactor temperature was maintained by

passing a water/ethylene glycol mixture through the jacket using a refrigerating/heating circulator set at the desired temperature. This polymerization system has been used extensively in our prior studies,[25,26] and a similar polymerization procedure is used herein. Prior to the polymerization, the reactor was cleaned carefully using toluene and acetone, purged with N_2 and heated overnight at 70 °C under vacuum, and then cooled to the desired temperature under N_2 protection. Chlorobenzene (280 mL) was then injected into the reactor under N_2 protection. Freshly prepared solution of catalyst **1** in chlorobenzene (20 mL, containing 0.32 mmol of catalyst) was subsequently injected into the reactor under N_2 protection. The solution was stirred for about 5 min to establish the equilibrium temperature. The reactor was then quickly pressurized to the prescribed ethylene pressure (1, 3, or 27 atm) to start the polymerization. During the course of polymerization, ethylene pressure was maintained constant by the continuous feed of ethylene from a cylinder, and the temperature was also controlled constant with the circulator. A prescribed volume of polymerization solution was sampled from the reactor sampling port every hour during the polymerization. At the end of polymerization, ethylene pressure was released and the reactor was emptied.

Each sampled solution was quenched by adding triethylsilane (ca. 0.5 mL) under stirring. After being stirred for about 1 h, the solvent was evaporated with the use of a stream of air to obtain the polymer product. In order to remove black Pd powder residues resulting from the deactivated Pd−diimine catalyst, the polymer product was redissolved in THF. HCl acid (37%, ca. 0.5 mL) and H_2O_2 solution (50 wt %, ca. 0.5 mL) were subsequently added into the solution under stirring. After stirring for 1 h, the polymer was precipitated in a large amount of methanol and was further washed with excess methanol until it was nearly colorless. Finally, the polymer sample was dried in vacuum at 70 °C overnight, weighed, and subsequently characterized.

General Procedure for Two- or Three-Stage Ethylene Polymerizations at Varying Conditions. The polymerizations (runs 5−10 shown in Tables 3−5, respectively) were carried out with the same reactor system used above. To the cleaned and N_2-protected reactor were added chlorobenzene (280 mL) and freshly prepared solution of catalyst **1** in chlorobenzene (20 mL, containing 0.32 mmol catalyst). The solution was stirred for 5 min to establish the desired temperature. The reactor was then quickly pressurized to the prescribed ethylene pressure to start the polymerization. At the end of the first stage of polymerization, ethylene pressure was quickly adjusted to the desired value for the second stage. Simultaneously, the reactor temperature was changed by switching to another refrigerating/heating circulator set at the desired temperature for the second stage. Generally, the desired ethylene pressure was achieved within 5 min after the end of the first stage, and the desired temperature was established within about 15 min. For the three-stage run (run 10 in Table 5) involving three different conditions, a similar change of the polymerization condition was made at the end of the second stage. During the course of each polymerization, polymerization solutions were sampled from the reactor sampling port generally at 1 h intervals. The procedure for polymer separation and purification is identical to the one used above.

Characterizations and Measurements. ^{13}C nuclear magnetic resonance (NMR) spectra of the polymers were obtained on a Bruker AV500 spectrometer at ambient temperature with $CDCl_3$ as the solvent. Polymer characterization with triple-detection gel permeation chromatography (GPC) was carried out on a Polymer Laboratories PL-GPC220 system equipped with a triple detection array, including a differential refractive index (DRI) detector (from Polymer Laboratories), a three-angle light scattering (LS) detector (high-temperature mini-DAWN from Wyatt Technology), and a four-bridge capillary viscometer (from Polymer Laboratories). The detection angles of the light scattering detector were 45°, 90°, and 135°, and the laser wavelength was 687 nm. One guard column (PL# 1110-1120) and three 30 cm columns (PLgel 10 μm MIXED-B 300 × 7.5 mm) were used. The use of this triple-detection GPC system for polymer characterization has been reported in our earlier works,[26,28c,28d,31f−31h] and a similar methodology is used herein.

HPLC-grade THF was used as the mobile phase at a flow rate of 1 mL/min. The complete GPC system, including columns and detectors, was maintained at 33 °C. The mass of the polymers injected into the column varied with polymer molecular weight; typically 200 μL of 5−7 mg/mL solution was injected. Astra software from Wyatt Technology was used for data collection and analysis. Two narrow polystyrene standards (from Pressure Chemicals) with weight-average molecular weight (M_w) of 30 and 200 kg/mol were used for the normalization of light scattering signals at the three angles and the determination of interdetector delay volume and band broadening, respectively. The DRI increment dn/dc value of 0.078 mL/g was used for all polyethylene samples synthesized herein,[26,27b,28c,28d,31f−31h] and the value of 0.185 mL/g was used for polystyrene. The two polystyrene standards were measured to have a typical M_w value of 30.8 and 205.2 kg/mol, respectively, with a polydispersity index (PDI) of 1.00 for both, which well match the data provided from the supplier.

Rheological characterization of the polymer melts was performed on a TA Instruments AR-G2 rheometer. A Peltier plate measurement configuration with a 20 mm parallel plate geometry at a gap size of 1.0 mm was used for the measurements. The measurements were all conducted in the small-amplitude dynamic oscillation mode within the frequency range of 0.001−100 Hz. A strain sweep was performed at 10 Hz before frequency sweeps to establish the linear viscoelastic region for each polymer. The measurements were performed at regular temperature intervals of 10 °C within a temperature range from 15 to 65 °C. Measurement temperature was maintained within ±0.1 °C by using the Peltier plate temperature control system. Time−temperature superposition of the rheological data was made by using data analysis software provided by TA Instruments.

Results and Discussion

Single-Stage Ethylene "Living" Polymerization. Our strategy in this one-pot synthesis of hyperbranched−linear block polyethylenes having hybrid block topologies is to vary the polymerization condition during the course of chain walking ethylene "living" polymerization catalyzed with a Pd−diimine catalyst, $[(ArN{=}C(Me){-}(Me)C{=}NAr)Pd(CH_3)(N{\equiv}CMe)]^+SbF_6^-$ (Ar = 2,6-(iPr)$_2$C$_6$H$_3$) (**1**). Given the chain walking mechanism of the Pd−diimine catalyst, a variation in condition (ethylene pressure and temperature) during the course of "living" polymerization is expected to result in a change in polymer chain topology and lead to the convenient construction of block polymers composed of topologically different polyethylene blocks. Meanwhile, a control of polymerization time at each condition should render the simple tuning of the length of each block. However, the key to the success of this synthesis is to maintain the "living" behavior of the polymerization despite the variation in polymerization condition in order to achieve the block structures. The occurrence of significant undesired chain breaking reactions (chain transfer and termination) caused by the variation in polymerization condition would lead to ill-defined polymers. Polymerization conditions, at which both topology tuning and "living" polymerization characteristics can be effectively achieved, should thus be screened out in designing the polymerizations.

For this purpose, we first carried out four single-stage ethylene polymerizations (runs 1−4 in Table 1) at four fixed conditions, respectively, without involving a variation of condition with catalyst **1**. These four runs are used here as

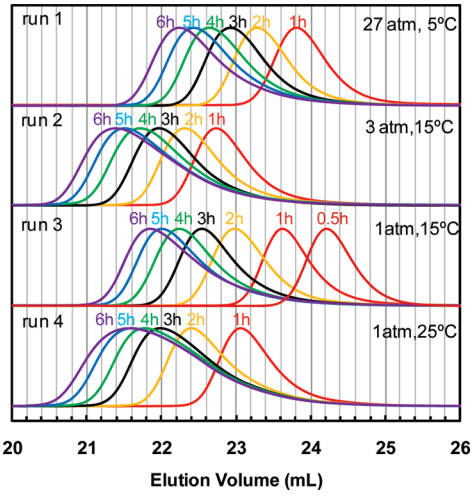

Figure 1. GPC elution traces (from DRI detector) for the four sets of control polymers synthesized via single-stage ethylene polymerizations (runs 1−4) at the four different combinations of ethylene pressure and temperature.

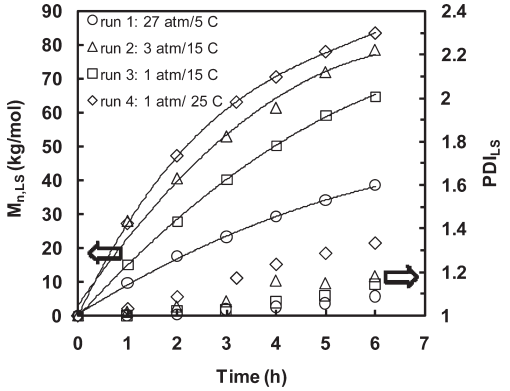

Figure 2. Dependencies of $M_{n,LS}$ and PDI_{LS} on polymerization time for the control polymers synthesized via single-stage ethylene polymerizations (runs 1−4) at the four different combinations of ethylene pressure and temperature.

the control experiments. The four conditions involve different combinations of ethylene pressure (1, 3, and 27 atm) and temperature (5, 15, and 25 °C): 27 atm/5 °C for run 1, 3 atm/15 °C for run 2, 1 atm/15 °C for run 3, and 1 atm/25 °C for run 4. We selected these four conditions to evaluate the effects of pressure and temperature on both polymer chain topology and, more importantly, the "living" polymerization characteristics. While the effects of pressure and temperature on polymer topology have been well demonstrated with more compact topology resulting at a lower pressure and/or a higher temperature,[27,28] their systematic effects on the "living" characteristics of the polymerization has not been investigated in detail. Among the four conditions, the combination of 27 atm/5 °C is the one commonly used in the literature[24] and in our previous studies[25a−c,26] to achieve "living" polymerization behavior with various Pd−diimine catalysts.

These single-stage polymerization runs were all undertaken for a total polymerization time of 6 h with samples taken generally every hour to monitor the polymerization behavior. The resulting polymers were subsequently characterized with triple-detection gel permeation chromatography (GPC) and melt rheometry to determine their molecular weight development and chain topology information. The triple-detection GPC incorporates a differential refractive index (DRI) detector, a three-angle light scattering (LS) detector, and a four-capillary viscometer, enabling the simultaneous determination of polymer absolute molecular weight and intrinsic viscosity. The GPC system was operated at 33 °C with THF as the mobile phase since all polymers have good solubility THF even at room temperature. Table 1 summarizes the polymerization results and the data from polymer characterization. Figure 1 shows the GPC elution traces obtained from the DRI detector for the polymers synthesized in the four runs. In each run, the polymer elution peaks move consistently toward the left (i.e., reduced elution volume) with the increase of polymerization time, indicating the continuous increase of polymer molecular weight with time. Meanwhile, a slight but increasingly pronounced broadening in the GPC elution peaks, along with an increasingly longer GPC tail at the high elution volume end, is also observed with the increase of polymerization time in each run, particularly in run 4 carried out at the highest temperature (25 °C). This suggests the presence of undesired chain breaking reactions (transfer and/or termination) in the polymerizations.

The molecular weight information on the polymers, including the absolute number- and weight-average molecular weights ($M_{n,LS}$ and $M_{w,LS}$) and polydispersity index (PDI_{LS}), were determined with the LS detector of the triple-detection GPC. The data are summarized in Table 1. In Figure 2, the dependencies of $M_{n,LS}$ and PDI_{LS} on polymerization time for all the four runs are demonstrated. In all the runs, $M_{n,LS}$ increases with polymerization time though not in a strictly linear pattern, along with the concomitant increase of the PDI_{LS} value. The nonlinear dependence of $M_{n,LS}$ on time and enhancement in PDI_{LS} are particularly pronounced in run 4 at the highest polymerization temperature (25 °C), while only negligibly affected by ethylene pressure (comparing runs 2 and 3). In run 1 at the lowest temperature of 5 °C, the PDI_{LS} values are generally below 1.09 within the 6 h of polymerization. In both runs 2 and 3 at 15 °C, the PDI_{LS} values are still below 1.18 after 6 h while the values in run 4 at 25 °C are significantly higher, with 1.17 at 3.2 h and 1.33 at 6 h. These results on polymer molecular weight development confirm the quasi-living polymerization feature in all the four runs within the polymerization time (6 h) with the presence of slight chain breaking reactions. The occurrence of such chain breaking reactions is sensitive to the increase of polymerization temperature while without obvious dependency on ethylene pressure. From Figure 1, the $M_{n,LS}$ value at a given polymerization time increases with pressure and temperature due to the enhanced chain propagation rate. Given the lower PDI values achieved in runs 1−3, the three associated conditions (27 atm/5 °C, 3 atm/15 °C, and 1 atm/15 °C) render better maintained "living" feature and are thus better suited for the subsequent synthesis of well-defined block polymers through stagewise polymerizations involving a variation of polymerization condition.

The chain topology of these narrow-distributed control polymers synthesized in the four runs is elucidated by evaluating their intrinsic viscosity ($[\eta]$) and zero-shear (or Newtonian) melt viscosity (η_0), along with their dependencies on molecular weight. As well demonstrated in our earlier studies,[28] both viscosity data depend sensitively on polymer chain topology, generally with reduced values found for polymers of more compact chain topologies at a given molecular weight. These viscosity data are summarized in Table 1. The intrinsic viscosity is determined herein in THF at 33 °C using the viscosity detector in triple-detection GPC measurement. Figure 3 plots the dependences of polymer weight-average intrinsic viscosity ($[\eta]_w$) on $M_{w,LS}$ (i.e., Mark−Houwink plot) for the four runs, which shows clearly

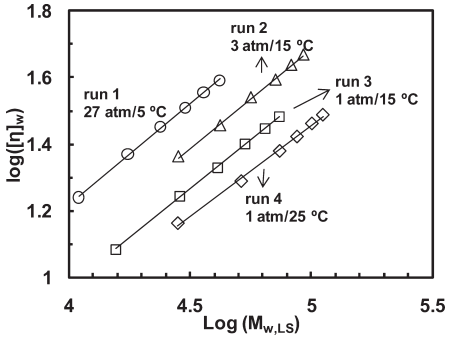

Figure 3. Mark−Houwink plot of the four sets of control polymers synthesized via single-stage ethylene polymerizations (runs 1−4) at the four different combinations of ethylene pressure and temperature. Linear fitting equations: run 1, $\log [\eta]_w = 0.603 \log M_w - 1.19$ ($R^2 = 0.999$); run 2, $\log [\eta]_w = 0.599 \log M_w - 1.31$ ($R^2 = 0.999$); run 3, $\log [\eta]_w = 0.589 \log M_w - 1.39$ ($R^2 = 1.00$); run 4, $\log [\eta]_w = 0.548 \log M_w - 1.28$ ($R^2 = 0.997$).

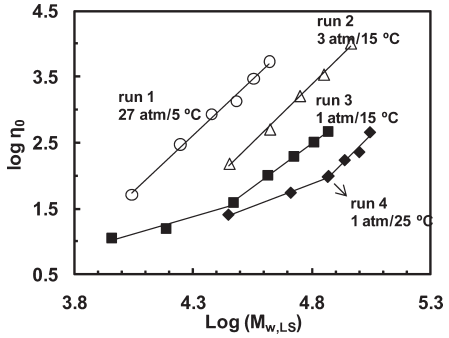

Figure 4. Dependencies of η_0 at 25 °C on $M_{w,LS}$ for the four sets of control polymers synthesized via single-stage ethylene polymerizations (runs 1−4) at the four different conditions. Linear fitting equations: run 1, $\log \eta_0 = 3.37 \log M_w - 11.9$ ($R^2 = 0.994$); run 2, $\log \eta_0 = 3.55 \log M_w - 13.7$ ($R^2 = 0.997$); run 3, $\log \eta_0 = 1.06 \log M_w - 3.18$ ($R^2 = 0.954$) when $M_w < M_c$ and $\log \eta_0 = 2.69 \log M_w - 10.4$ ($R^2 = 0.999$) when $M_w > M_c$; run 4, $\log \eta_0 = 1.39 \log M_w - 4.81$ ($R^2 = 0.996$) when $M_w < M_c$ and $\log \eta_0 = 3.57 \log M_w - 15.4$ ($R^2 = 0.956$) when $M_w > M_c$.

the topological differences among the polymers synthesized in the four runs. Consistent with the chain walking mechanism, reducing ethylene pressure and/or enhancing temperature from run 1 to 4 lead to reduced intrinsic viscosity at a given molecular weight (i.e., increasingly hyperbranched chain topology), which is reflected as the continuous downshift of the intrinsic viscosity curves in Figure 3.[28] The four intrinsic viscosity curves are nearly parallel in the plot with the Mark−Houwink exponent (α) decreasing slightly from about 0.600 in runs 1 and 2, to 0.589 in run 3, and to 0.548 in run 4. Though slight, this reduction of the α value from run 1 to 4 is also indicative of the increasingly enhanced chain compactness as polymers of compact chain topologies (such as dendrimers and star polymers) often exhibit lower α values.[26b]

Given the highest ethylene pressure and the lowest temperature employed, the polymers synthesized in run 1 should possess the least compact chain topology among the four sets due to the shortest catalyst chain walking distance at this condition.[27,28] On the basis of our previous studies,[25a−c,26,28] these polymers should possess linear chain topology with primarily short branching structures on the linear backbone. To quantify the chain topology differences among the four sets of polymers, we use herein the contraction factor (g'), defined as the ratio of intrinsic viscosity of a polymer in runs 2−4 to that of linear reference polymer of equal molecular weight synthesized at the condition of 27 atm/5 °C in run 1 (calculated through the fitting equation $[\eta] = 0.064M^{0.603}$ shown in Figure 3). In the calculation, the polymers in run 1 are used as the reference due to their least compact linear topology among the four sets of polymers. The calculated g' values are also listed in Table 1. Typically, the g' values are 0.73, 0.55, and 0.43 for those in runs 2−4, respectively, indicating quantitatively the successful achievement of topology tuning with the four different conditions.

The polymer melts were characterized with small-amplitude dynamic oscillation rheometry in the temperature range of 15−65 °C. The zero-shear melt viscosity at 25 °C was obtained by performing time−temperature superposition on the complex viscosity data with the reference temperature of 25 °C. All the polymer melts have been found to be thermorheologically simple, well obeying time−temperature superposition with a very similar flow activation energy (E_a) of about 45 kJ/mol found for all polymers (see Table 1). Figure 4 plots the dependences of η_0 at 25 °C on $M_{w,LS}$ for the polymers synthesized in the four runs, which further demonstrates clearly the topological differences among the polymers. With the reduction of ethylene pressure and/or the increase of temperature from run 1 to 4, there is a continuous downshift of the zero-shear viscosity curve, indicating the zero-shear viscosity at a given molecular weight is reduced significantly resulting from the increasing chain compactness.[28a,b] Moreover, there is a unique transition involved in the dependency of η_0 on polymer molecular weight for runs 3 and 4, which represents the critical entanglement molecular weight (M_c). Traditionally, the dependency of zero-shear melt viscosity on polymer molecular weight is correlated by the power law $\eta_0 = KM^b$, where the value of the exponent b is approximately 1.0 for polymers with molecular weight below M_c and is about 3.4 above M_c.[32,33] The transition around M_c is often sharp and represents the onset of chain entanglements. Generally, M_c is about 2 times the entanglement molecular weight (M_e).[32,33] However, it has been shown that dendrimers do not have M_c due to the absence of chain entanglements as a result of their unique dendritic structures.[34] This power-law relationship has been confirmed to hold for a broad variety of linear polymer systems.[32,33] Herein, the narrow polydispersity of these control polymers enables us to determine directly their unique relationships between η_0 and molecular weight and, moreover, the dependency of such relationships on chain topology.

For polymers in runs 1 and 2 herein, there is no transition found within the investigated molecular weight ranges with the value of b being 3.37 and 3.55 (Figure 4), respectively, which are very close to 3.4 found with many linear polymers. Therefore, the molecular weights of these polymers in runs 1 and 2 should be well above their respective M_c values, which could not be determined herein given the unavailability of polymers of significantly lower molecular weights. On the basis of the transitions observed in Figure 4, the M_c value for the polymers synthesized in runs 3 and 4 is estimated to be about 28 and 87 kg/mol, respectively. These values are much greater than the typical value of about 2 kg/mol found for linear polyethylenes,[32] demonstrating the compact hyperbranched chain topology in these polymers. Meanwhile, the higher value in run 4 than in run 3 further confirms the more hyperbranched topology for the polymers synthesized in run 4 at 25 °C.[35−37] For the polymers in run 3, the b value is 1.06 below M_c, close to 1.0 found for linear polymers, and is 2.69 above M_c, which somehow deviates from 3.4 for linear polymers. For those in run 4, the b value is 1.39 below M_c, deviating slightly from 1.0, and is 3.57 above M_c.

Branching structures in some selected polymers synthesized in these control experiments were analyzed with ^{13}C NMR spectroscopy. Because of the limitation of the ^{13}C NMR technique, only short branches with length below six carbons can be distinguished, and details on branch-on-branch structures, i.e., chain topology, cannot be obtained.[27,28] Representatively, Table 2 lists the short branching distribution of three polymers of very similar $M_{n,LS}$ (about 28 kg/mol): the 4 h sample in run 1, 1 h sample in run 2, and 2 h sample in run 3. Despite their significant differences in chain topology as reflected from their intrinsic viscosity and zero-shear viscosity data, these three polymers have similar total short branching density (about 100 per 1000 carbons) and branching distribution, which is in consistency with our prior studies.[28]

These four single-stage control runs thus confirm solidly the successful achievements of both distinctly different chain topologies and the "living" polymerization feature at the four different conditions. Given the better maintained "living" polymerization behavior with lower polymer PDI values found in runs 1−3, the three conditions involving the lower temperatures, 27 atm/5 °C, 3 atm/15 °C, and 1 atm/15 °C, are thus more suited for the subsequent synthesis of block polymers with hybrid topologies through two- or three-stage "living" polymerizations. We use Scheme 1 to depict schematically the chain topology differences among the polymers synthesized at these three conditions in runs 1−3.

Two-Stage "Living" Polymerizations for Synthesis of Diblock Polyethylenes Containing Two Blocks of Different Topologies. Two-stage ethylene "living" polymerizations with the two stages carried out at two different conditions (runs 5−7 in Table 3; runs 8 and 9 in Table 4) were then carried out to synthesize diblock polyethylenes containing two blocks of different chain topologies. Representatively, we chose herein two conditions, 27 atm/5 °C and 1 atm/15 °C, to demonstrate the versatility of this synthesis since the polymers produced at these two conditions differ greatly in topology (linear and hyperbranched, respectively). As will be illustrated below, the order of the growth of the blocks (i.e., "hyperbranched-first" or "linear-first") is found to be critical herein, with the order of "hyperbranched-first" being required in order to obtain successfully the distinct hybrid block structure. During each two-stage polymerization, ethylene pressure and temperature were changed swiftly to the second condition to start the second-stage polymerization following immediately the completion of the first-stage polymerization at the first condition for a prescribed period of time. Generally, the required ethylene pressure and temperature for the second stage were established within 5 and 15 min, respectively, after the completion of the first stage.

Table 2. Short Chain Branching Distribution (in Number of Branches per 1000 Carbons) of the Polymers Determined with ^{13}C NMR Spectroscopy

run	time (h)	methyl	ethyl	propyl	butyl	amyl	hexyl+	total	% B[a]
1	4	37.7	17.3	3.8	8.6	3.7	27.2	98.3	12
2	1	34.0	21.5	2.6	6.5	3.0	31.8	99.4	17
3	2	34.2	22.3	2.2	6.9	2.4	34.1	102.1	19

[a] Percentage of methyl from *sec*-butyl branches in the total methyl.

Table 3 summarizes the results for the "hyperbranched-first" two-stage polymerizations (runs 5−7) with the first stage at 1 atm/15 °C and the second stage at 27 atm/5 °C. The first-stage polymerization time (t_1) varied from 1 h for run 5 to 3 h for run 7 to obtain the first hyperbranched block of different sizes. In each run, a sample was taken at the end of the first stage to obtain the first-stage polymer. The second stage lasted for 5 h in total in each run, with samples taken at every hour (i.e., different second-stage time t_2) to obtain different sizes for the second linear block and, moreover, monitor its growth. The polymer samples were characterized with triple-detection GPC and melt rheometry, with the results listed in Table 3. With this growth order of "hyperbranched-first", treelike hyperbranched−linear block structure with a hyperbranched corona and a linear trunk should result, with the second linear block being extended from the hyperbranched first block in the second stage (see Scheme 2a). Because of the short chain walking distance at the second-stage condition (27 atm/5 °C), the catalyst should be prevented from walking back to the first hyperbranched block during the growth of the second linear block, leading to distinct hyperbranched−linear block structure. However, slight catalyst chain walking into the first block may still occur at the very beginning of the second stage when the second block is too short, and thus the separation of the two blocks is not clearly defined.[24b] Despite this, the joint of the two blocks should be in close vicinity to the location where the catalyst situates at the end of the first stage, and it may differ among chains given the statistical nature of both chain walking and growing processes.

Figure 5a shows the GPC elution traces of the polymers collected in the three "hyperbranched-first" two-stage runs. The first-stage polymer sampled at the end of the first stage (i.e., $t_2 = 0$ h) in each run is also included for comparison. In each run, the elution peaks of second-stage polymers (i.e., block polymers) remain monomodal and move continuously

Scheme 1. Synthesis of Narrow-Distributed Polyethylenes of Different Chain Topologies via Single-Step Ethylene "Living" Polymerization with the Pd−Diimine Catalyst at Three Respective Conditions

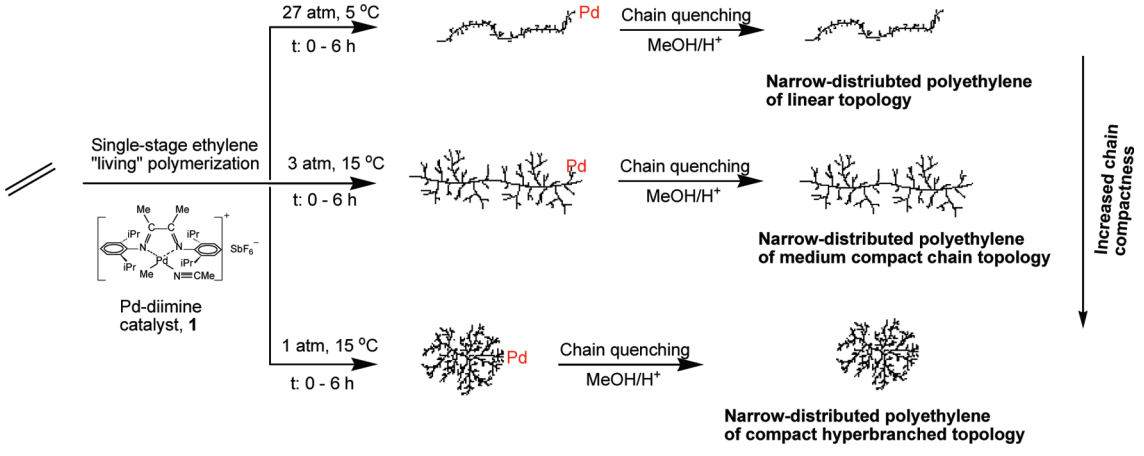

Table 3. "Hyperbranched-First" Two-Stage Ethylene "Living" Polymerizations (Runs 5−7) Using Catalyst 1 with the First Stage at 1 atm/15 °C and the Second Stage at 27 atm/5 °C and Polymer Characterization Results with Triple-Detection GPC and Melt Rheometry

				triple-detection GPC characterization[b]					number-average block size			melt rheometry characterization[d]	
run	1st-stage time t_1 (h)	2nd-stage time t_2[a] (h)	polymer productivity (kg/(mol Pd h)	$M_{n,LS}$ (kDa)	$M_{w,LS}$ (kDa)	PDI_{LS}	$[\eta]_w$ (mL/g)	g'	1st block (kDa)	2nd block (kDa)	calculated $[\eta]_w$[c] (mL/g)	η_0 (25 °C) (Pa s)	E_a (kJ/mol)
5	1	0	14	15.7	15.7	1.00	12.1	0.56	15.7	0		18	45
		1	9.4	23.3	23.4	1.01	19.1	0.69		7.6	19.1	89	46
		2	8.6	29.5	30.0	1.01	24.5	0.76		13.8	24.3	312	48
		3	6.3	34.3	35.6	1.04	28.7	0.80		18.6	28.3	921	49
		4	7.2	39.1	41.5	1.06	32.7	0.84		23.4	32.1	2299	50
		5	7.8	42.8	47.3	1.10	36.4	0.86		27.1	35.7	4540	51
6	2	0	11	21.9	22.0	1.01	13.6	0.51	21.9	0		25	46
		1	13	31.9	32.6	1.02	22.3	0.66		10.0	23.2	177	46
		2	9.7	36.3	37.8	1.04	26.6	0.72		14.4	26.9	523	48
		3	9.2	41.9	43.8	1.04	30.9	0.76		20.0	30.8	1476	48
		4	7.9	45.9	49.4	1.08	34.6	0.80		24.0	34.3	3074	50
		5	8.9	48.7	53.5	1.10	37.3	0.82		26.8	36.7		
7	3	0	11	34.8	35.6	1.02	17.9	0.50	34.8	0		55	45
		1	11	41.8	43.3	1.03	23.9	0.60		7.0	24.9	164	46
		2	10	46.4	49.0	1.06	28.5	0.66		11.6	28.7	555	48
		3	9.2	49.7	53.8	1.08	31.8	0.70		14.9	31.5	1347	47
		4	9.0	53.6	58.8	1.10	35.2	0.73		18.8	34.5	2529	49
		5	9.4	57.5	64.1	1.11	38.3	0.75		22.7	37.5	3956	49

[a] Other polymerization conditions: amount of catalyst **1**, 0.32 mmol; solvent, chlorobenzene; total volume, 300 mL. [b] Number-average molecular weight ($M_{n,LS}$), weight-average molecular weight ($M_{w,LS}$), and polydispersity index (PDI_{LS}) are absolute values determined using the light scattering detector in triple-detection GPC. Weight-average intrinsic viscosity ($[\eta]_w$) data were measured using the online viscometer. The contraction factor (g') is defined as the ratio of intrinsic viscosity of the polymer to that of linear polymer of equal molecular weight synthesized at 27 atm and 5 °C. The fitting equation ($\log [\eta]_w = 0.603 \log M_w - 1.19$) shown in Figure 3 is used for the calculation of the intrinsic viscosity of linear reference polymers of equal molecular weight. [c] The calculated $[\eta]_w$ is obtained by using Ho-Duc and Prud'homme's combination rule.[38] The weight fractions of the hyperbranched first block and linear second block are calculated through the $M_{w,LS}$ data of the first-stage polymer and block polymer. The $[\eta]_w$ data of the hyperbranched block and linear block having the same molecular weight of the block polymer are calculated by using the corresponding Mark−Houwink equations constructed in Figure 3. [d] Polymer melt rheological characterization was conducted in the small-amplitude dynamic oscillation mode within the linear viscoelastic region. The zero shear viscosity η_0 at 25 °C and flow activation energy (E_a) were obtained by evaluating the rheological data measured in the temperature range of 15−65 °C with time−temperature superposition.

Table 4. "Linear-First" Two-Stage Ethylene "Living" Polymerizations (Runs 8 and 9) Using Catalyst 1 with the First Stage at 27 atm/5 °C and the Second Stage at 1 atm/15 °C and Polymer Characterization Results with Triple-Detection GPC and Melt Rheometry

				triple-detection GPC characterization[b]						melt rheometry characterization[d]	
run	1st-stage time t_1[a] (h)	2nd-stage time t_2 (h)	polymer productivity (kg/(mol Pd h)	$M_{n,LS}$ (kDa)	$M_{w,LS}$ (kDa)	PDI_{LS}	$[\eta]_w$ (mL/g)	g'	calculated $[\eta]_w$[c] (mL/g)	η_0 (25 °C) (Pa s)	E_a (kJ/mol)
8	1	0	8.8	10.4	10.5	1.00	16.5	0.97		37	41
		1	11	23.9	24.2	1.01	19.6	0.69	20.8	92	46
		2	12	37.2	38.1	1.02	22.7	0.61	24.7	150	45
		3	11	45.8	48.2	1.05	25.0	0.58	27.3	215	47
		4	10	54.9	58.2	1.06	27.2	0.57	29.8	310	46
		5	11	60.8	66.5	1.09	29.1	0.56	31.7	391	47
9	2	0	9.1	18.3	18.7	1.02	22.9	0.95		230	47
		1	10	29.1	29.8	1.02	24.2	0.75	26.4	275	47
		2	10	37.0	38.5	1.04	25.6	0.68	28.3	301	47
		3	10	46.0	48.5	1.05	27.4	0.64	30.6	369	47
		4	9.5	54.1	58.1	1.07	29.0	0.61	32.7	505	49
		5	9.7	61.1	66.4	1.09	30.6	0.59	34.4		

[a] Other polymerization conditions: amount of catalyst **1**, 0.32 mmol; solvent, chlorobenzene; total volume, 300 mL. [b] Number-average molecular weight ($M_{n,LS}$), weight-average molecular weight ($M_{w,LS}$), and polydispersity index (PDI_{LS}) are absolute values determined using the light scattering detector in triple-detection GPC. Weight-average intrinsic viscosity ($[\eta]_w$) data were measured using the online viscometer. The contraction factor (g') is defined as the ratio of intrinsic viscosity of the polymer to that of linear polymer of equal molecular weight synthesized at 27 atm and 5 °C. The fitting equation ($\log [\eta]_w = 0.603 \log M_w - 1.19$) shown in Figure 3 is used for the calculation of the intrinsic viscosity of linear reference polymers of equal molecular weight. [c] The calculated $[\eta]_w$ is obtained by using Ho-Duc and Prud'homme's combination rule.[38] The weight fractions of the hypothetical linear first block and hyperbranched second block are calculated through the $M_{w,LS}$ data of the first-stage polymer and block polymer. The $[\eta]_w$ data of the hypothetical hyperbranched block and linear block having the same molecular weight of the block polymer are calculated by using the corresponding Mark−Houwink equations constructed in Figure 3. [d] Polymer melt rheological characterization was conducted in the small-amplitude dynamic oscillation mode within the linear viscoelastic region. The zero shear viscosity η_0 at 25 °C and flow activation energy (E_a) were obtained by evaluating the rheological data measured in the temperature range of 15−65 °C with time−temperature superposition.

to the left with the increase of t_2 from 0 to 5 h despite the drastic variation in polymerization condition. Like the single-stage control runs, slight but increasingly pronounced broadening is also found with these two-stage runs during the progress of the polymerization. Figure 5b shows the dependencies of $M_{n,LS}$ and PDI_{LS} on t_2. The increase of $M_{n,LS}$ is significant in the second stage in each run though not in a strictly linear pattern. In all three runs, the PDI_{LS} values are maintained low, below 1.10 for all the polymers. These molecular weight data confirm the successful chain extension with the "living" growth of the second linear block from the first hyperbranched block in the second stage to

Scheme 2. Two-Stage Ethylene "Living" Polymerizations with Two Different Orders of the Growth of the Blocks (a) "Hyperbranched-First" and (b) "Linear-First"

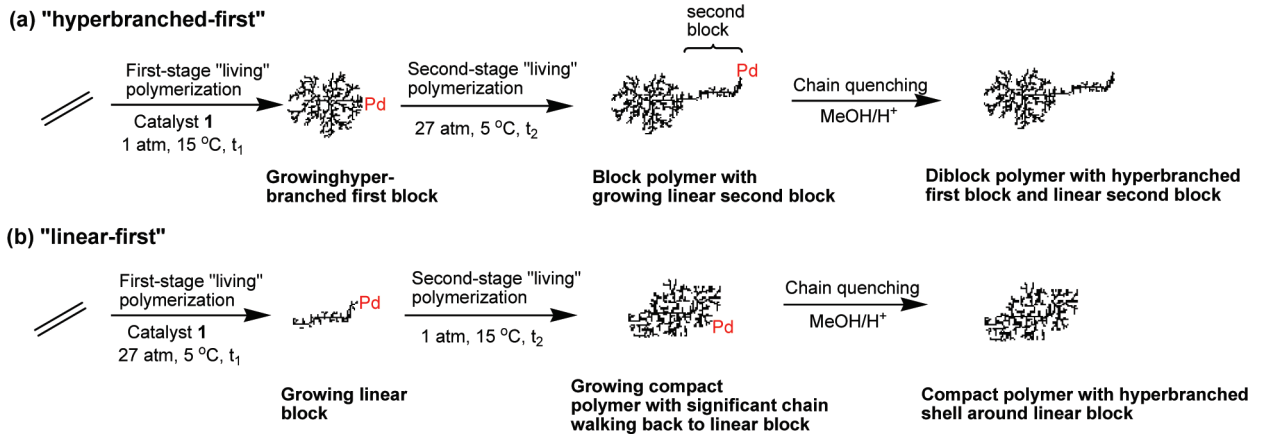

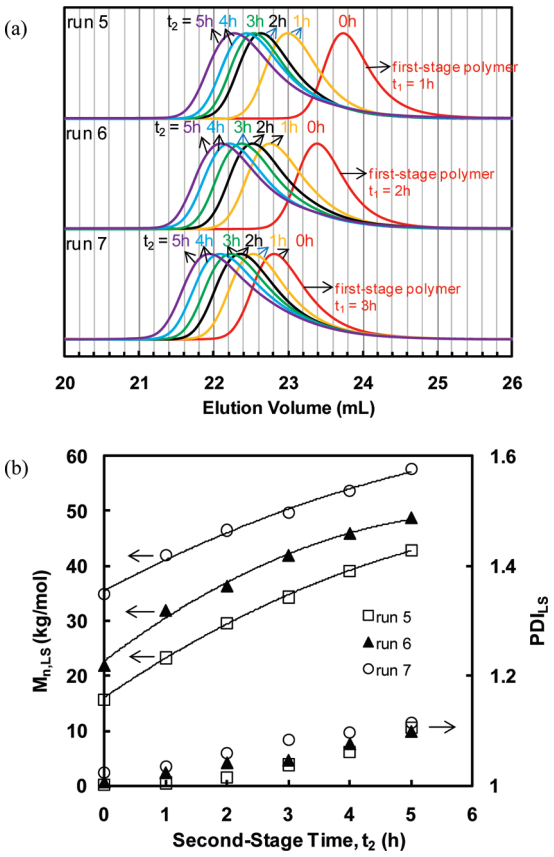

Figure 5. (a) GPC elution traces (from DRI detector) and (b) dependencies of $M_{n,LS}$ and PDI_{LS} on second-stage polymerization time for the three sets of polymers synthesized via "hyperbranched-first" two-stage ethylene polymerizations (runs 5−7).

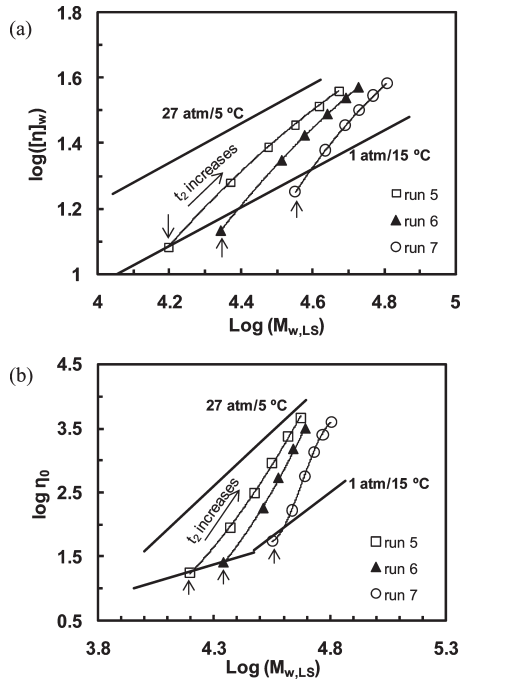

Figure 6. (a) Mark−Houwink plot and (b) dependencies of η_0 at 25 °C on $M_{w,LS}$ for the three sets of polymers synthesized via "hyperbranched-first" two-stage ethylene polymerizations (runs 5−7). The data points marked with an arrow represent first-stage polymers sampled at the end of the first stage.

form hyperbranched−linear diblock polymer. In each diblock polymer, the size of the hyperbranched block should be approximately the molecular weight of the first-stage polymer, and the size of the linear block can be calculated by subtracting the molecular weight of the diblock polymer with that of the hyperbranched first block. The number-average block size data are listed in Table 3. Tuning the polymerization time in each stage can thus control the size of each block given the versatile "living" nature of this two-stage polymerization.

The intrinsic viscosity data of these polymers in THF at 33 °C were determined with the viscosity detector of triple-detection GPC. Figure 6a shows the dependencies of $[\eta]_w$ on M_w for the polymers collected in the three runs, wherein the Mark−Houwink curves (obtained in Figure 3) for the control polymers synthesized in single-stage runs 1 and 3 are also included for comparison. As expected, the first-stage polymers in all the three runs have their intrinsic viscosity located on or close to the Mark−Houwink curve for the control polymers synthesized at 1 atm/15 °C, with slight deviations caused possibly by small unavoidable variations in polymerization condition (primarily ethylene pressure) from run to run. With the increase of t_2 in each run, the polymer intrinsic viscosity increasingly deviates from the curve for hyperbranched control polymers at 1 atm/15 °C and approaches to the one for the linear control polymers synthesized at 27 atm/5 °C. The g' values for the polymers in the three runs, relative to the linear control polymers synthesized at 27 atm/5 °C, were calculated (listed in Table 3). In each run, the g' value increases continuously with the increase of t_2 due to the

increasing size of the second linear block. For instance, in run 6, g' increases from 0.51 for first-stage hyperbranched polymer (t_2 = 0 h) to 0.66 at t_2 of 2 h, to 0.76 at t_2 of 3 h, and to 0.82 at t_2 of 5 h (Table 3).

The intrinsic viscosity of linear diblock (AB) and symmetric triblock (ABA) copolymers in a good or theta solvent for both A and B blocks has been found by Ho-Duc and Prud'homme to obey the following combination rule:[38]

$$[\eta]^{2/3} = \omega_a[\eta]_a^{2/3} + (1-\omega_a)[\eta]_b^{2/3} \quad (1)$$

where ω_a and $1-\omega_a$ are the weight fractions of A and B blocks, respectively, and $[\eta]_a$ and $[\eta]_b$ are the respective intrinsic viscosity of A and B homopolymers having equal molecular weight as the block copolymer. The hyperbranched−linear diblock polyethylenes synthesized herein through the "hyperbranched-first" two-stage "living" polymerizations are found to interestingly follow this combination rule as well. In Table 3, the intrinsic viscosity data calculated using eq 1 for the block polymers are also listed. In the calculation, the weight fractions of the hyperbranched first block and linear second block were determined by using the $M_{w,LS}$ data of the block polymer and the corresponding first-stage polymer, and the intrinsic viscosity data for the homopolymers having equal molecular weight were obtained through the Mark−Houwink equations shown in Figure 3. In all the three runs, the calculated intrinsic viscosity data are in good agreement with the corresponding measured ones, indicating the validity of this combination rule for these novel hyperbranched−linear block polymers. Moreover, this further provides solid evidence proving the presence of the distinct hybrid hyperbranched−linear jointed diblock structure in these polymers. On the basis of the low polymer PDI data, the size of each block in the diblock polymers should be narrow distributed.

Figure 6b plots the zero-shear melt viscosity at 25 °C of the polymers synthesized in the three "hyperbranched-first" runs as a function of their $M_{w,LS}$. Similar to the behavior of their intrinsic viscosity data, the zero-shear melt viscosity of the polymers in each run departs away from the curve for the hyperbranched control polymers synthesized at 1 atm/15 °C and approaches quickly toward that for the linear control polymers at 27 atm/5 °C with the increase of t_2 from 1 to 5 h. Once again, this confirms the increasing extension of the second linear block, which leads to more linear overall chain topology and enhances significantly the zero-shear viscosity of the polymers.

To contrast with the above "hyperbranched-first" runs, two "linear-first" two-stage "living" polymerizations (runs 8 and 9 in Table 4) were also carried out with the growth of the linear block first. In these two runs, the first stage was performed at 27 atm/5 °C for t_1 of 1 h (run 8) or 2 h (run 9) to grow the first linear block, followed with the second stage at 1 atm/15 °C for a total of 5 h. Similarly, samples were taken at the end of first stage and every hour during the second stage. Table 4 summarizes the results of polymerization and polymer characterization. With this order of growth of the blocks, we hypothesized that significant catalyst chain walking back to the first linear block should occur due to the long chain walking distance at 1 atm/15 °C. Instead of growing a distinct second hyperbranched block, the chain growth in the second stage would likely occur around the first linear block because of the long and random catalyst walking, rendering a shell of hyperbranched segments surrounding the linear block (Scheme 2b).[24b] The resulting polymers thus should not have a distinct linear−hyperbranched block structure and this "linear-first" order would be ineffective for the purpose of synthesis of block polymers having hybrid topologies.

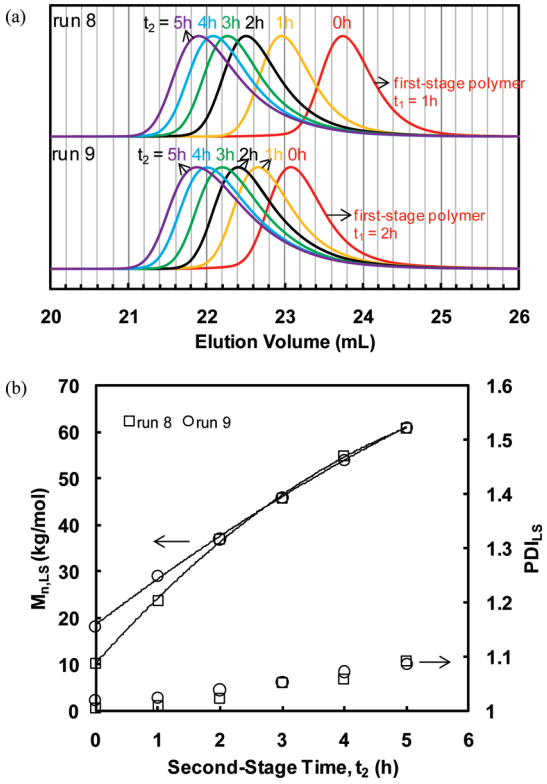

Figure 7. (a) GPC elution traces (from DRI detector) and (b) dependencies of $M_{n,LS}$ and PDI_{LS} on second-stage polymerization time for the two sets of polymers synthesized via "linear-first" two-stage ethylene polymerizations (runs 8 and 9).

Figure 7a shows the GPC elution traces of the polymers collected in the two "linear-first" runs. Similarly, the peaks move continuously to the left in each run with the increase of t_2 in the second stage, accompanied by slight but increasingly pronounced broadening at the low-molecular-weight end. The $M_{n,LS}$ data as a function of t_2 shown in Figure 7b, along with the low PDI values (below 1.10), indicate the maintained "livingness" of these two polymerizations despite the different order of growth compared to the above "hyperbranched-first" runs. Figure 8a plots the intrinsic viscosity data of the polymers in the two runs, with those of the corresponding control polymers for comparison. Opposite to the polymers synthesized via the "hyperbranched-first" order, the intrinsic viscosity data in each run depart from the curve for the linear control polymers synthesized at 27 atm/5 °C and approach to that for the hyperbranched control polymers synthesized at 1 atm/15 °C with the increase of t_2. In each run, the g' value decreases continuously with the increase of t_2 (see Table 4), demonstrating the increasingly compact chain topology. For example, in run 8, the first-stage polymer (t_2 = 0 h) has a g' value of 0.97 while those obtained at a t_2 of 1, 3, and 5 h have the g' values of 0.69, 0.58, and 0.56, respectively. In particular, the latter two g' values are very close to that (0.55) for hyperbranched control polymers synthesized at 1 atm/15 °C, thus demonstrating their similarly highly compact chain topology.

To verify our hypothesis of the absence of the distinct linear−hyperbranched block structures in these "linear-first" two-stage polymers, we also employed eq 1 to estimate their intrinsic viscosity data. In using the equation, we assumed the presence of the block structure with the size of the linear block equal to the molecular weight of the first-stage polymer and the size of the hyperbranched block determined by subtracting the overall molecular weight with that of the linear block. The intrinsic

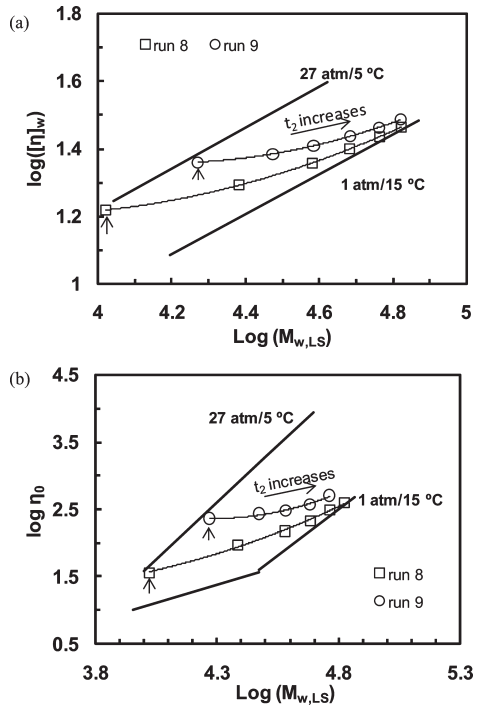

Figure 8. (a) Mark−Houwink plot and (b) dependencies of η_0 at 25 °C on $M_{w,LS}$ for the two sets of polymers synthesized via "linear-first" two-stage ethylene polymerizations (runs 8 and 9). The data points marked with an arrow represent first-stage polymers sampled at the end of the first stage.

viscosity data of the two blocks were also calculated with the Mark−Houwink equations obtained in Figure 3. The calculated intrinsic viscosity data are listed in Table 4. One can see that the measured intrinsic viscosity for each two-stage polymer in the two runs is significantly lower than the corresponding calculated ones. This is in sharp contrast to the block polymers synthesized above with the "hyperbranched-first" order and indicates their more compact chain topology compared to true hyperbranched−linear hybrid block polymers. This comparison of the intrinsic viscosity data provides the evidence supporting the absence of the distinct block structures in the two-stage polymers obtained with this "linear-first" order.

Figure 8b plots the zero-shear melt viscosity of the polymers synthesized in the two "linear-first" runs at different t_2. Compared to those shown in Figure 6b for block polymers synthesized with the "hyperbranched-first" order, much lower zero-shear viscosity values along with much weaker dependency on polymer molecular weight can be found. As an example, we illustrate the difference between the "hyperbranched-first" two-stage polymer synthesized in run 7 at t_2 = 4 h (overall M_n = 53.6 kg/mol with a hyperbranched first block of M_n = 34.8 kg/mol and a linear second block of M_n = 18.8 kg/mol) and the "linear-first" two-stage polymer synthesized in run 9 at t_2 = 4 h (overall M_n = 54.1 kg/mol with the first stage linear block of M_n = 18.3 kg/mol and the M_n increase of 35.8 kg/mol in the second stage at 1 atm/15 °C). These two samples have very similar overall M_n (53.6 and 54.1 kg/mol, respectively), the size for the linear block grown at 27 atm/5 °C (18.8 and 18.3 kg/mol, respectively), and the size grown at 1 atm/15 °C (34.8 and 35.8 kg/mol, respectively). However, the difference in their zero-shear viscosity is nearly 5 times, with 2529 Pa s for the "hyperbranched-first" one in run 7 and 505 Pa s for the "linear-first" one in run 9. This distinct difference in zero-shear viscosity further confirms the significant difference in chain topologies among the polymers synthesized with the two different orders and the need of "hyperbranch-first" for obtaining distinct block structures.

Three-Stage "Living" Polymerization for Synthesis of Triblock Polyethylenes Containing Three Blocks of Different Topologies. To further demonstrate the versatility of this facile polymerization technique, we extend its use for the synthesis of triblock polyethylenes containing three hybrid blocks of varying topologies by three-stage "living" polymerization at three sequential conditions: 1 atm/15 °C, 3 atm/15 °C, and 27 atm/5 °C. To successfully obtain the triblock structure by minimizing chain walking back to the previous block, the order of the growth of blocks in the three-stage polymerization, in reference to above two-stage polymerization results, should start with the first block having the most compact topology (corresponding to longest catalyst walking distance), followed consecutively with the second block having the medium compact topology (medium walking distance) and the third block having the most linear topology (shortest walking distance). As a demonstration, we conducted herein a three-stage run (run 10 summarized in Table 5), with the first stage at 1 atm/15 °C for 1 h (t_1), the second stage at 3 atm/15 °C for 1 h (t_2), and the third stage at 27 atm/5 °C for a total of 4 h (t_3). The polymerization conditions were varied in this specific sequence to reduce consecutively catalyst walking distance and to introduce sequentially the blocks of increasing linearness in topology (see Scheme 3). During the course of polymerization, samples were taken at the ends of first and second stages and every hour during the third stage to monitor the block growth. The polymerization results and polymer characterization data are summarized in Table 5.

Parts a and b of Figure 9 show respectively the GPC elution traces of the polymers sampled during the polymerization and the development of $M_{n,LS}$ and PDI_{LS} as functions of polymerization time. Like the above two-stage runs, continuous increase of $M_{n,LS}$ with maintained low PDI_{LS} values (below 1.10) is also achieved during this three-stage run, demonstrating again the facile "living" behavior of this Pd−diimine-catalyzed polymerization despite the involvement of three drastically different conditions. The size of each block in the triblock polymers obtained at different t_3 is estimated from the molecular weight data of the first- and second-stage polymers and the triblock polymers. In the estimation, the first-stage polymer is considered to constitute the first block and the size of the second block is the molecular weight difference between the first- and second-stage polymers. The size of the third linear block at different t_3 is calculated by subtracting the molecular weight of corresponding triblock polymer with that of the second-stage polymer. The estimated number-average sizes of the blocks are summarized in Table 5. This estimation is based on the assumption that there is no overlap among the blocks and the separation between two consecutive blocks is clear. However, some catalyst chain walking back to the previous block is expected to occur particularly in the beginning of the second stage at 3 atm/15 °C, at which the chain walking distance should be significantly longer compared to that in the third stage at 27 atm/5 °C. Therefore, the separation between the first and second block should not be as clear as that seen in the diblock polymers synthesized in "hyperbranched-first" two-stage runs 5−7.

Figure 10a shows the development of $[\eta]_w$ as a function of $M_{w,LS}$ during the progress of the three-stage polymerization, wherein the three Mark−Houwink curves for the respective control polymers synthesized at the conditions are also included for comparison. With the introduction of the second and third stages, the intrinsic viscosity curve moves up

Table 5. Three-Stage Ethylene "Living" Polymerization Using Catalyst 1 (Run 10) with the First Stage at 1 atm/15 °C, the Second Stage at 3 atm/15 °C, and the Third Stage at 27 atm/5 °C, and Polymer Characterization Results with Triple-Detection GPC and Melt Rheometry

				triple-detection GPC characterization[b]					number-average block size				melt rheometry characterization[d]	
1st-stage time t_1 (h)	2nd-stage time t_2 (h)	3rd-stage time t_3[a] (h)	polymer productivity (kg/(mol Pd h)	$M_{n,LS}$ (kDa)	$M_{w,LS}$ (kDa)	PDI_{LS}	$[\eta]_w$ (mL/g)	g'	1st block (kDa)	2nd block (kDa)	3rd block (kDa)	calculated $[\eta]_w$[c] (mL/g)	η_0 (25 °C) (Pa s)	E_a (kJ/mol)
1	0	0	12	14.8	15.3	1.04	12.0	0.56	14.8	0	0		15	42
	1	0	16	32.4	33.4	1.03	21.6	0.63		17.6	0	22.2	131	45
	1	1	14	38.7	39.9	1.03	27.8	0.73		17.6	6.3	26.7	509	47
	1	2	12	42.7	45.2	1.06	31.6	0.77		17.6	10.3	30.2	1336	49
	1	3	9.9	47.3	50.4	1.06	34.9	0.79		17.6	14.9	33.4	2537	50
	1	4	9.6	51.8	56.0	1.08	38.3	0.82		17.6	19.4	36.7	5126	51

[a] Other polymerization conditions: amount of catalyst **1**, 0.32 mmol; solvent, chlorobenzene; total volume, 300 mL. [b] Number-average molecular weight ($M_{n,LS}$), weight-average molecular weight ($M_{w,LS}$), and polydispersity index (PDI_{LS}) are absolute values determined using the light scattering detector in triple-detection GPC. Weight-average intrinsic viscosity ($[\eta]_w$) data were measured using the online viscometer. The contraction factor (g') is defined as the ratio of intrinsic viscosity of the polymer to that of linear polymer of equal molecular weight synthesized at 27 atm and 5 °C. The fitting equation ($\log [\eta]_w = 0.603 \log M_w - 1.192$) shown in Figure 3 is used for the calculation of the intrinsic viscosity of linear reference polymers of equal molecular weight. [c] The calculated $[\eta]_w$ is obtained by using Ho-Duc and Prud'homme's combination rule.[38] The weight fraction of each block is calculated through the $M_{w,LS}$ data of the first-stage polymer, second-stage polymer, and the triblock polymer. The $[\eta]_w$ value of each block having the same molecular weight of the block polymer is calculated by using the corresponding Mark−Houwink equations constructed in Figure 3. [d] Polymer melt rheological characterization was conducted in the small-amplitude dynamic oscillation mode within the linear viscoelastic region. The zero shear viscosity η_0 at 25 °C and flow activation energy (E_a) were obtained by evaluating the rheological data measured in the temperature range of 15−65 °C with time−temperature superposition.

Scheme 3. Three-Stage Ethylene "Living" Polymerization

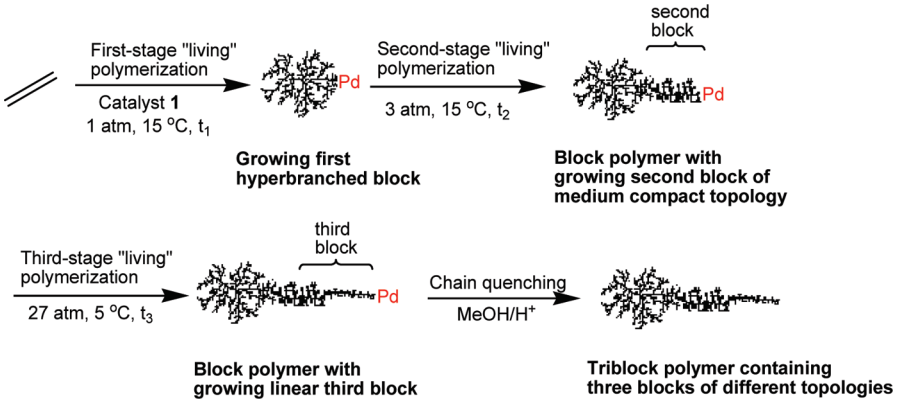

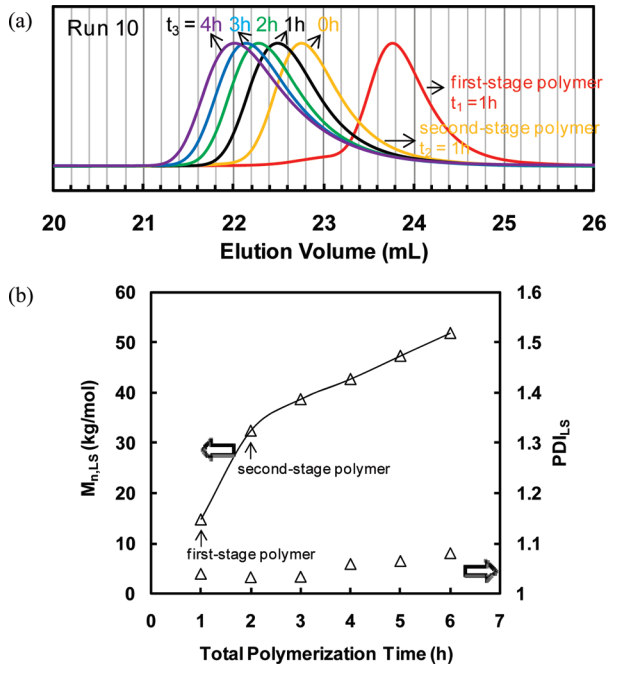

Figure 9. (a) GPC elution traces (from DRI detector) and (b) dependencies of $M_{n,LS}$ and PDI_{LS} on polymerization time for the set of polymers synthesized via three-stage ethylene polymerization (run 10).

continuously and approaches toward the curve for linear control polymers synthesized at 27 atm/5 °C, indicating the increasing overall chain linearness due to the incorporation and/or extension of the more linear second and third blocks. A similar trend is also found from the zero-shear melt viscosity data shown in Figure 10b. We have also attempted to use the combination rule of Ho-Duc and Prud'homme to estimate the intrinsic viscosity of the diblock polymer obtained at the end of the second stage and the triblock polymers obtained during the third stage at different t_3 (1−4 h). To be used for the triblock polymers, the equation is expanded to have three terms with each corresponding to one block, i.e.

$$[\eta]^{2/3} = \omega_a[\eta]_a^{2/3} + \omega_b[\eta]_b^{2/3} + (1-\omega_a-\omega_b)[\eta]_c^{2/3} \quad (2)$$

where ω_a, ω_b, and $1-\omega_a-\omega_b$ are the mass fractions of the three respective A, B, and C blocks. The calculated $[\eta]_w$ data are listed in Table 5. For the second-stage polymer, the calculated $[\eta]_w$ is 22.2 mL/g and is slightly greater than the measured one of 21.6 mL/g (Table 5), indicating the presence of the speculated overlapping between the first and second blocks. For the triblock polymers obtained during the third stage at different t_3, the calculated data are consistently slightly lower than the corresponding measured data, which is opposite to our expectation considering the presence of nonclear separation between the

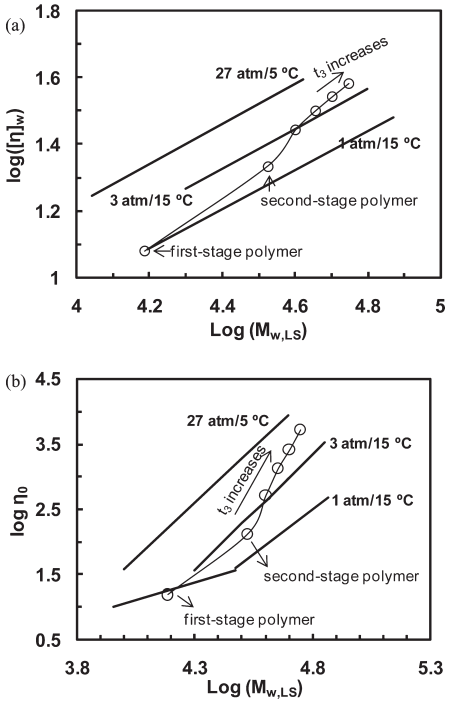

Figure 10. (a) Mark−Houwink plot and (b) dependency of η_0 at 25 °C on $M_{w,LS}$ for the set of polymers synthesized via three-stage ethylene polymerization (run 10).

blocks. This inconsistency may possibly be attributed to the insuitability of the extension of this combination rule to ABC triblock polymers despite its validity for diblock and ABA-type triblock polymers.

Conclusions

The synthesis of a novel range of diblock and triblock polyethylenes constructed with chemically identical chain blocks of hybrid hyperbranched−linear topologies is demonstrated in this work using stagewise chain walking ethylene "living" polymerization with catalyst **1** at varying conditions. This unique one-pot synthetic technique benefits from the remarkable features of the Pd−diimine catalyst in ethylene polymerization: the versatile "living" polymerization characteristics over a broad range of ethylene pressure/temperature and the convenient tunability of polymer chain topology by the change of ethylene pressure/temperature. Three polymerization conditions, 27 atm/5 °C, 3 atm/15 °C, and 1 atm/15 °C, have been representatively chosen herein for use in the stagewise "living" polymerization. With the "hyperbranched-first" order of block growth, narrow-distributed hyperbranched−linear diblock polymers with distinct block structure of controllable block sizes and low PDI (below 1.10) have been obtained with the first polymerization stage at 1 atm/15 °C and the second stage at 27 atm/5 °C. The presence of the distinct block structure in these diblock polymers is confirmed on the basis of their intrinsic viscosity data, which fit well with the combination rule identified for common diblock polymers. On the contrary, the "linear-first" order of block growth, with the first stage at 27 atm/5 °C and the second at 1 atm/15 °C, is instead unsuccessful to achieve the hybrid block structure due to significant catalyst chain walking back to the previous linear block in the second polymerization stage, demonstrating the importance of the growth order of the blocks in this synthetic technique. In addition, triblock polymers composed of blocks of increasing topological linearness are also obtained by varying the condition sequentially from 1 atm/15 °C to 3 atm/15 °C and to 27 atm/5 °C. Not restricted to the diblock and triblock polymers demonstrated herein, this facile polymerization technique can be extended to the synthesis of a class of block polymers composed of different numbers of blocks and/or combination of block topologies by using desirable polymerization conditions, which are not limited to the three used herein.

Acknowledgment. The financial support from the Natural Science and Engineering Research Council (NSERC) of Canada is greatly appreciated. Z.Y. also thanks NSERC and the Canadian Foundation for Innovation (CFI) for funding research equipment and facilities.

References and Notes

(1) See representative review articles: (a) Pyun, J.; Zhou, X.-Z.; Drockenmuller, E.; Hawker, C. J. *J. Mater. Chem.* **2003**, *13*, 2653. (b) Hawker, C. J.; Wooley, K. L. *Science* **2005**, *309*, 1200. (c) Hedrick, J. L.; Magbitang, T.; Connor, E. F.; Glauser, T.; Volksen, W.; Hawker, C. J.; Lee, V. Y.; Miller, R. D. *Chem.—Eur. J.* **2002**, *8*, 3309.

(2) See representative review articles on dendrimers: (a) Tomalia, D. A.; Fréchet, J. M. J. *J. Polym. Sci., Part A: Polym. Chem.* **2002**, *40*, 2719. (b) Grayson, S. M.; Fréchet, J. M. J. *Chem. Rev.* **2001**, *101*, 3819.

(3) See representative review articles on hyperbranched polymers: (a) Voit, B. I.; Lederer, A. *Chem. Rev.* **2009**, *109*, 5924. (b) Gao, C.; Yan, D. *Prog. Polym. Sci.* **2004**, *29*, 183.

(4) See representative review articles on star polymers: (a) Hadjichristidis, N.; Pitsikalis, M.; Pispas, S.; Iatrou, H. *Chem. Rev.* **2001**, *101*, 3747. (b) Blencowe, A.; Tan, J. F.; Goh, T. K.; Qiao, G. G. *Polymer* **2009**, *50*, 5. (c) Higashihara, T.; Sugiyama, K.; Yoo, H.-S.; Hayashi, M.; Hirao, A. *Macromol. Rapid Commun.* **2010**, *12*, 1031.

(5) See a representative review article on cyclic polymers: Kricheldorf, H. R. *J. Polym. Sci., Part A: Polym. Chem.* **2010**, *48*, 251.

(6) See a representative review article on hybrid dendritic−linear polymers: Gitsov, I. *J. Polym. Sci., Part A: Polym. Chem.* **2008**, *46*, 5295.

(7) (a) Gitsov, I.; Fréchet, J. M. J. *Macromolecules* **1993**, *26*, 6536. (b) Gitsov, I.; Fréchet, J. M. J. *Macromolecules* **1994**, *27*, 7309. (c) Gillies, E. R.; Jonsson, T. B.; Fréchet, J. M. J. *J. Am. Chem. Soc.* **2004**, *126*, 11936.

(8) Gitsov, I.; Zhu, C. *J. Am. Chem. Soc.* **2003**, *125*, 11228.

(9) Magbitang, T.; Lee, V. Y.; Cha, L. N.; Wang, H.-L.; Chung, W. R.; Miller, R. D.; Dubois, G.; Volksen, W.; Kim, H.-C.; Hedrick, J. L. *Angew. Chem., Int. Ed.* **2005**, *44*, 7574.

(10) (a) Johnson, M. A.; Iyer, J.; Hammond, P. T. *Macromolecules* **2004**, *37*, 2490. (b) Nguyen, P. M.; Hammond, P. T. *Langmuir* **2006**, *22*, 7825. (c) Nguyen, P. M.; Zacharia, N. S.; Verploegen, E.; Hammond, P. T. *Chem. Mater.* **2007**, *19*, 5524. (d) Tian, L.; Hammond, P. T. *Chem. Mater.* **2006**, *18*, 3976.

(11) Namazi, H.; Adeli, M. *J. Polym. Sci., Part A: Polym. Chem.* **2005**, *43*, 28.

(12) Zhou, Z.; D'Emanuele, A.; Lennon, K.; Attwood, D. *Macromolecules* **2009**, *42*, 7936.

(13) Leolukman, M.; Paoprasert, P.; Mandel, I.; Diaz, S. J.; Mcgee, D. J.; Gopalan, P. *J. Polym. Sci., Part A: Polym. Chem.* **2009**, *47*, 5017.

(14) (a) Lee, E.; Lee, B.-I.; Kim, S.-H.; Lee, J.-K.; Zin, W.-C.; Cho, B.-K. *Macromolecules* **2009**, *42*, 4134. (b) Cho, B.-K.; Kim, S.-H.; Lee, E. *J. Polym. Sci., Part A: Polym. Chem.* **2010**, *48*, 2372.

(15) (a) del Barrio, J.; Oriol, L.; Alcalá, R.; Sánchez, C. *Macromolecules* **2009**, *42*, 5752. (b) del Barrio, J.; Oriol, L.; Sánchez, C.; Serrano, J. L.; Di Cicco, A.; Keller, P.; Li, M.-H. *J. Am. Chem. Soc.* **2010**, *132*, 3762.

(16) Desai, A.; Atkinson, N.; Rivera, F. J.; Devonport, W.; Rees, I.; Branz, S. E.; Hawker, C. J. *J. Polym. Sci., Part A: Polym. Chem.* **2000**, *38*, 1033.

(17) Chang, Y.; Kwon, Y. C.; Lee, S. C.; Kim, C. *Macromolecules* **2000**, *33*, 4496.

(18) (a) Barriau, E.; Marcos, A. G.; Kautz, H.; Frey, H. *Macromol. Rapid Commun.* **2005**, *26*, 862. (b) Marcos, A. G.; Pusel, T. M.; Thomann, R.; Pakula, T.; Okrasa, L.; Geppert, S.; Gronski, W.; Frey, H. *Macromolecules* **2006**, *39*, 971.

(19) (a) Leduc, M. R.; Hawker, C. J.; Dao, J.; Fréchet, J. M. J. *J. Am. Chem. Soc.* **1996**, *118*, 11111. (b) Leduc, M. R.; Hayes, W.; Fréchet, J. M. J. *J. Polym. Sci., Part A: Polym. Chem.* **1998**, *36*, 1.

(20) Mecerreyes, D.; Dubois, Ph.; Jérôme, R.; Hedrick, J. L.; Hawker, C. J. *J. Polym. Sci., Part A: Polym. Chem.* **1999**, *37*, 1923.

(21) Al-Muallem, H. A.; Knauss, D. M. *J. Polym. Sci., Part A: Polym. Chem.* **2001**, *39*, 152.
(22) Patton, D. L.; Taranekar, P.; Fulghum, T.; Advincula, R. *Macromolecules* **2008**, *41*, 6703.
(23) Lang, A. S.; Kogler, F. R.; Sommer, M.; Wiesner, U.; Thelakkat, M. *Macromol. Rapid Commun.* **2009**, *30*, 1243.
(24) (a) Gottfried, A. C.; Brookhart, M. *Macromolecules* **2001**, *34*, 1140. (b) Gottfried, A. C.; Brookhart, M. *Macromolecules* **2003**, *36*, 3085.
(25) (a) Zhang, Y.; Ye, Z. *Chem. Commun.* **2008**, 1178. (b) Zhang, K.; Ye, Z.; Subramanian, R. *Macromolecules* **2008**, *41*, 640. (c) Zhang, Y.; Ye, Z. *Macromolecules* **2008**, *41*, 6331. (d) Li, S.; Ye, Z. *Macromol. Chem. Phys.* **2010**, *17*, 1917.
(26) (a) Zhang, K.; Ye, Z.; Subramanian, R. *Macromolecules* **2009**, *42*, 2313. (b) Xia, X.; Ye, Z.; Morgan, S.; Lu, J. *Macromolecules* **2010**, *43*, 4889.
(27) (a) Guan, Z.; Cotts, P. M.; McCord, E. F.; McLain, S. J. *Science* **1999**, *283*, 2059. (b) Cotts, P. M.; Guan, Z.; McCord, E.; McLain, S. *Macromolecules* **2000**, *33*, 6945. (c) Guan, Z. *Chem.—Eur. J.* **2002**, *8*, 3086.
(28) (a) Ye, Z.; Zhu, S. *Macromolecules* **2003**, *36*, 2194. (b) Ye, Z.; AlObaidi, F.; Zhu, S. *Macromol. Chem. Phys.* **2004**, *205*, 897. (c) Xiang, P.; Ye, Z.; Morgan, S.; Xia, X.; Liu, W. *Macromolecules* **2009**, *42*, 4946. (d) Morgan, S.; Ye, Z.; Subramanian, R.; Wang, W.-J.; Ulibarri, G. *Polymer* **2010**, *51*, 597.
(29) (a) Ittel, S. D.; Johnson, L. K.; Brookhart, M. *Chem. Rev.* **2000**, *100*, 1169. (b) Johnson, L. K.; Killian, C. M.; Brookhart, M. *J. Am. Chem. Soc.* **1995**, *117*, 6414. (c) Johnson, L. K.; Mecking, S.; Brookhart, M. *J. Am. Chem. Soc.* **1996**, *118*, 267. (d) Mecking, S.; Johnson, L. K.; Wang, L.; Brookhart, M. *J. Am. Chem. Soc.* **1998**, *120*, 888.
(30) (a) Chen, G.; Ma, X. S.; Guan, Z. *J. Am. Chem. Soc.* **2003**, *125*, 6697. (b) Chen, G.; Guan, Z. *J. Am. Chem. Soc.* **2004**, *126*, 2662. (c) Chen, G.; Huynh, D.; Felgner, P. L.; Guan, Z. *J. Am. Chem. Soc.* **2006**, *128*, 4298. (d) Sun, G.; Guan, Z. *Macromolecules* **2010**, *43*, 4829.
(31) (a) Ye, Z.; Li, S. *Macromol. React. Eng.* **2010**, *5*, 319. (b) Zhang, K.; Wang, J.; Subramanian, R.; Ye, Z.; Lu, J.; Yu, Q. *Macromol. Rapid Commun.* **2007**, *28*, 2185. (c) Wang, J.; Ye, Z.; Joly, H. *Macromolecules* **2007**, *40*, 6150. (d) Wang, J.; Ye, Z.; Zhu, S. *Ind. Eng. Chem. Res.* **2007**, *46*, 1174. (e) Wang, J.; Kontopoulou, M.; Ye, Z.; Subramanian, R.; Zhu, S. *J. Rheol.* **2008**, *52*, 243. (f) Morgan, S.; Ye, Z.; Zhang, K.; Subramanian, R. *Macromol. Chem. Phys.* **2008**, *209*, 2232. (g) Ye, J.; Ye, Z.; Zhu, S. *Polymer* **2008**, *49*, 3382. (h) Wang, J.; Zhang, K.; Ye, Z. *Macromolecules* **2008**, *41*, 2290. (i) Xu, L.; Ye, Z.; Cui, Q.; Gu, Z. *Macromol. Chem. Phys.* **2009**, *210*, 2194. (j) Xiang, P.; Ye, Z. *Macromol. Rapid Commun.* **2010**, *31*, 1083.
(32) Graessley, W. W. *Adv. Polym. Sci.* **1974**, *16*, 1.
(33) Hiemenz, P. C.; Lodge, T. P. *Polymer Chemistry*, 2nd ed.; CRC Press: Boca Raton, FL, 2007.
(34) Hawker, C. J.; Farrington, P. J.; Mackay, M. E.; Wooley, K. L.; Fréchet, J. M. J. *J. Am. Chem. Soc.* **1995**, *117*, 4409.
(35) Ye, Z.; Feng, W.; Zhu, S.; Yu, Q. *Macromol. Rapid Commun.* **2006**, *27*, 871.
(36) Rose, J. M.; Cherian, A. E.; Lee, J. H.; Archer, L. A.; Coates, G. W.; Fetters, L. J. *Macromolecules* **2007**, *40*, 6807.
(37) Patil, R.; Colby, R. H.; Read, D. J.; Chen, G.; Guan, Z. *Macromolecules* **2005**, *38*, 10571.
(38) Ho-Duc, N.; Prud'homme, J. *Macromolecules* **1973**, *6*, 472.